Available online at www.sciencedirect.com
ScienceDirect
International Journal of Heat and Mass Transfer 51 (2008) 4535–4543
International Journal of HEAT and MASS TRANSFER
www.elsevier.com/locate/ijhmt

Friction factor and heat transfer in multiple microchannels with uniform flow distribution

Hee Sung Park *, Jeff Punch

Stokes Research Institute, University of Limerick, Ireland

Received 15 December 2006
Available online 8 April 2008

Abstract

Predictions of flow and heat transfer in microchannels are ongoing issues in microfludics. This work focused on laminar flow ($69 < Re < 800$) within rectangular microchannel with hydraulic diameter from 106 μm to 307 μm for single-phase liquid flow. The friction factors obtained by experiments on the microchannels showed that conventional theory for fully-developed flow is applicable within the range of our experiments. A manifold configuration which ensured uniform flow through the microchannel array is thought to contribute to the improvement of accuracy. The average Nusselt number for the microchannel array was also evaluated experimentally in the condition of constant heat transfer rate. We found that there were deviations between the experimental and theoretical values of heat transfer rate in the microchannels. In order to predict heat transfer rate accurately, we proposed an empirical correlation in terms of $Nu/(Re^{0.62}\,Pr^{0.33})$ and Brinkman number confined to the experimental range. The correlation is expected to be useful to design the microchannel devices related to heat transfer.

Keywords: Microchannels; Friction factor; Heat transfer; Manifold; Brinkman number

1. Introduction

Microscale fluidic technologies have revolutionized many aspects of applied sciences and engineering, such as microflow sensors, pumps, valves, thin film coating, heat exchangers, combustors, fuel processors, and biomedical and biochemical analysis instruments [1,2]. The use of microchannels has become common in these applications. Many scientific and engineering programmes have been conducted to develop more effective and sophisticated devices. Fundamental investigations of the friction factor and heat transfer rate in microchannels have been conducted by many researchers, generally using theoretical values developed from Navier–Stokes equations and energy equation. For practical applications, accurate correlations for friction factor and heat transfer which is backed with physical understanding are significant. One of the authors' previously published papers showed an example of determining the optimum microchannel dimensions for electronic device cooling by using correlation equations [3].

Wu and Cheng [4] obtained a correlation between Poiseuille number and the aspect ratio in a trapezoidal silicon microchannel. They ascribed Poiseuille number as less than or greater than 16, depending on the aspect ratio. Steinke and Kandlikar [5] reviewed previous studies addressing the topic of fluid flow and heat transfer and tried to explain the deviation in data by conducting experiments. They concluded that deviations came from the measurement uncertainty of microchannel dimensions, in conjunction with inlet and exit losses. Koo and Kleinstreuer [6] proposed that the viscous effects should be taken into consideration for experimental and computational analyses. Kohl et al. [7] measured the internal pressure within microchannels by using microfabricated pressure sensors. They noted that over- or under-estimation of pressure drops was caused by increased pressure drop in entrance region of the channel.

* Corresponding author. Tel.: +353 61 233722; fax: +353 61 202393.
E-mail addresses: heros93@naver.com, heesung.park@ul.ie (H.S. Park).

0017-9310/$ - see front matter © 2008 Elsevier Ltd. All rights reserved.
doi:10.1016/j.ijheatmasstransfer.2008.02.009

Nomenclature

A	fin area
Br	Brinkman number, $\mu V^2/k\Delta T$
C_f	fanning friction factor
C_f^d	friction factor from developing flow
C_{f_exp}	friction factor obtained by experiment
C_{f_the}	friction factor obtained by theory
c_p	specific heat
D_c	channel width
D_d	channel depth
D_h	hydraulic diameter of channel
D_w	channel wall thickness
G	geometric parameter
h	heat transfer coefficient
k	thermal conductivity
K_∞	incremental pressure drop number
L	heat exchanger length
L_c	manifold length in contraction region
L_b	manifold length in parallel region
N_c	number of channel
Nu	Nusselt number, hD_h/k
Re	Reynolds number, $\rho V D_h/\mu$
Po	Poiseuille number, $C_f Re$
Pr	Prandtl number, $\mu c_p/k$
q	heat flux
T_m	bulk mean temperature
T_i	average inlet temperature
T_o	average outlet temperature
T_w	temperature at the wall wetted by water
V	mean velocity of water
W	heat exchanger width
x^+	hydraulic entrance length
x^*	thermal entrance length

Greek symbols

α	aspect ratio of channel
ρ	density of water
μ	viscosity
μ_w	viscosity at the wall
ΔP	pressure drop
ΔP_{man}	pressure drop in manifold
ΔP_{exp}	pressure drop measured in experiment
ΔT	$T_w - T_m$

Bayraktar and Pidugu [8] concluded, in their review paper, that experimental results on pressure drop and friction factor measurements reported in the literature are mostly inconsistent and contradictory. Hetsroni et al. [9] conducted experimentation on microchannel heat transfer rate and found that flow instabilities caused pressure fluctuation which decreased the heat transfer rate. Harm et al. [10] analyzed their experimental data assuming developing flow conditions, concluding that convective heat transfer theory was applicable. They indicated the importance of manifold design in microchannel arrays in order to ensure uniform flow distribution. The numerical calculations reported by Lee et al. [11] were compared with their experimental data, and it was found that a conventional analysis approach could be employed in predicting heat transfer behavior in microchannels. Hetsroni et al. [12] investigated the possible sources of unexpected phenomena in heat transfer experiments. They discussed the microscale effects of geometry, axial heat flux and energy dissipation, and indicated the significances of axial conduction, evaluation of temperatures and thermal entry length. Tso and Mahulikar [13] investigated the effect of viscous dissipation in microchannel heat transfer and suggested the dependence of $Nu/(Re^{0.62}Pr^{0.33})$ on Brinkman number which originated from Peng et al. [14].

From the review of published papers, large scatter is evident in measuring data for friction factor and heat transfer, and explanations are contradictory [8,12]. Meanwhile, recent papers have indicated that conventional theory is applicable by careful evaluation of geometry [5] or by considering other effects [12]. Specifically, many previous experimental studies were conducted by using multiple numbers of channels in test sections without showing the manifold condition. Non-uniform distribution of flow in the multiple channels can cause significant distortion on the analyses of experimental data for friction factor and heat transfer.

In this paper, experimental and theoretical analyses were carried out on a range of microchannel arrays with uniform flow distribution in order to determine accurate correlations for friction factor and heat transfer. A manifold geometry was created to ensure uniform inlet flow for each microchannel, and the friction factor and heat transfer rate were experimentally investigated and then compared with theory. The experimental results of the friction factor showed an excellent agreement with conventional hydraulic theory. We also analyzed the Nusselt number obtained from our experiments by using the correlation of $Nu/(Re^{0.62}Pr^{0.33})$ and proposed a correlation between heat transfer rate and Brinkman number.

2. Theoretical

The schematic diagram of a representative microchannel heat exchanger is presented in Fig. 1. Heat flux (q) is applied from the vertical direction through the upper plate of thickness (t). The channel dimensions are expressed with channel width (D_c), channel depth (D_d), wall thickness (D_w) between the channels, and overall width (W) and length (L).

2.1. Friction factor in a microchannel

The present work concerns the single-phase laminar flow in microchannels. The well-known Fanning friction factor

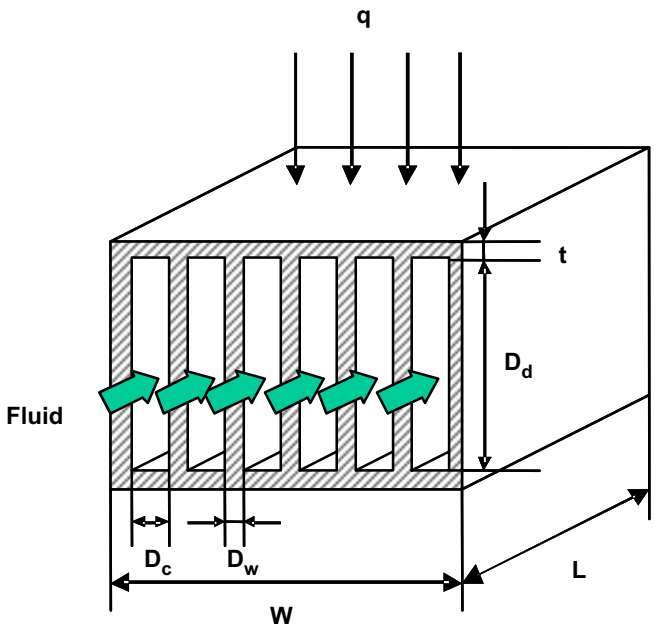

Fig. 1. Schematic of microchannel heat exchanger.

(C_f), defined in Eq. (1) accounts for the microchannel flow friction caused by wall shear stress

$$C_f = \frac{(\Delta P/L)D_h}{2\rho V^2} \tag{1}$$

$$D_h = \frac{2D_d D_c}{D_d + D_c} \tag{2}$$

where ΔP is pressure drop across the channel, D_h is the hydraulic diameter defined in Eq. (2), and ρ, V represent density and mean velocity of the liquid flow, respectively. For fully-developed laminar flow, the Poiseuille number is a function of channel aspect ratio, $\alpha = D_w/D_d$ [15,16]. Eq. (3) expresses the friction factor in terms of the geometric parameter, G, defined by Bejan [17,18].

$$C_f Re = 4.7 + 19.64G \tag{3}$$

$$G = \frac{\alpha^2 + 1}{(\alpha + 1)^2} \tag{4}$$

Hydrodynamically developing flow is quite important for microchannel flow analysis due to the short length of the microchannel [5,10]. From Kays and Crawford [16], a good approximate approximation for development flow length is expressed in

$$x^+ = \frac{x}{ReD_h} \tag{5}$$

Fully-developed flow is assumed valid above the value of $x^+ = 0.05$ [16]. The correction of friction factor for every range of x^+ value can be found in Ref. [10].

$$C_f^d = \frac{(\mu_w/\mu)^{0.58} 16/(0.67 + 0.46\alpha(2-\alpha)) - K_\infty/4x^+}{Re},$$
$$K_\infty = -0.906\alpha^2 + 1.693\alpha + 0.649, \quad x^+ \geqslant 0.1 \tag{6}$$

$$C_f^d = 11.3(x^+)^{-0.202}\alpha^{-0.094}, \quad 0.02 \leqslant x^+ < 0.1 \tag{7}$$

$$C_f^d = 5.26(x^+)^{-0.434}\alpha^{-0.01}, \quad 0.001 < x^+ < 0.02 \tag{8}$$

The function K_∞, the incremental pressure drop number, is a correlation of results obtained from an integral analysis of developing flow [10]. For the fully-developed and developing flow regions, the pressure drops for the given flow rates across the channel can be evaluated using the calculated friction factor.

2.2. Heat transfer in a microchannel

The heat transfer coefficient, h, which is significant for microscale heat exchanger design, can be obtained from the Nusselt number using the following:

$$h = \frac{kNu}{D_h} \tag{9}$$

Assuming a fully-developed temperature profile with constant heat flux, the Nusselt number is expressed in Eq. (10) as a function of geometric parameter, G [18]. The correlation shows good agreement with the analytical results of Kays and Crawford [16]

$$Nu = -1.047 + 9.326G \tag{10}$$

When the fluid temperature upstream of some point is assumed to be uniform and equal to the surface temperature, there is no heat transfer in this region [19]. Following this point, heat transfer which takes place is concerned with the development of the temperature profile. In the developing temperature profile, a heat transfer solution can be obtained by defining the thermal entrance length [16]

$$x^* = \frac{x}{ReD_h Pr} \tag{11}$$

where x^* and Pr represent thermal entrance length and Prandtl number, respectively. The average Nusselt number obtained by fitting the data from Shah and London [20] is shown in [19]

$$Nu = \left[\{2.22(x^*)^{-0.33}\}^3 + \{-0.02 + 8.31G\}^3\right]^{1/3} \tag{12}$$

It is evident from the literature that although conventional theory predicts friction factor accurately, significant discrepancies exist for heat transfer. In this paper, a novel heat transfer correlation is proposed, based on experimental data measured for microchannel arrays with uniform flow distribution.

3. Experiments

A range of rectangular shaped microchannels were fabricated by chemical wet etching ⟨110⟩ silicon wafer of 500 μm thickness. The details of the fabrication processes for the microchannels and heaters are shown in Fig. 2. The silicon wafer was then anodically bonded with 500 μm Pyrex glass plate in order to minimize heat loss.

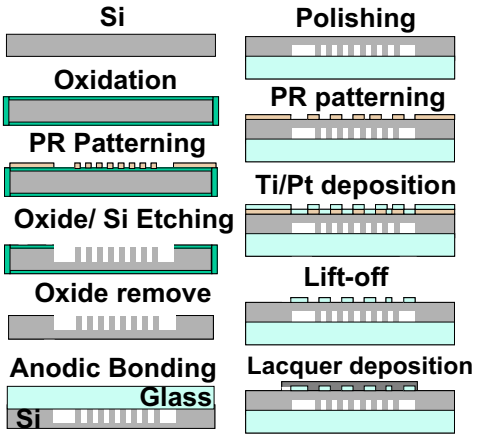

Fig. 2. Fabrication process for microchannel heat exchangers.

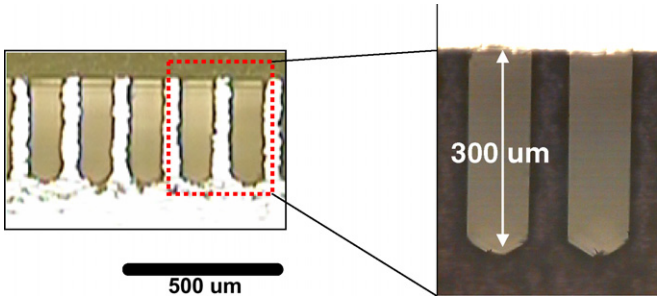

Fig. 3. Cross-sectional view of microchannel photographed by optical microscope.

A Pt/Ti thin film heater layer of 0.4 μm thickness was deposited on the backside of the silicon wafer. The total electrical resistance of the heater was 190 Ω. Finally, a black lacquer was coated over the thin film layer to measure the temperature profile using infra-red thermography. A cross-sectional view of a typical microchannel is shown in Fig. 3. Finally, each of the microchannel arrays was cut to 10 mm × 10 mm to ensure the same effective heating area.

At the completion of testing, the microchannel arrays were cross-sectioned in order to examine the dimension and shape using optical microscopy. As shown in Fig. 4, since there were no significant undercuts or unexpected deformations, analysis based on the rectangular shaped microchannel is thought to be valid. The measured microchannel dimensions are presented in Table 1, where the

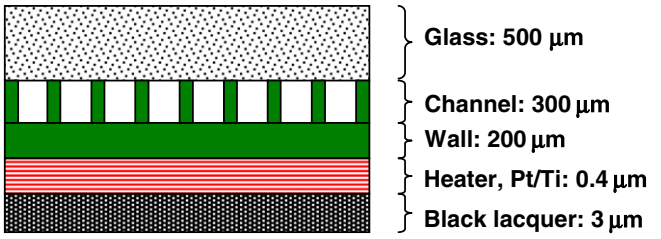

Fig. 4. Layers of microchannel heat exchanger fabricated for the experimentation.

microchannels were classified into two groups: the channel widths of the first group were varied from 65 μm to 315 μm, while the second group had same channel width of 100 μm but with varying numbers of channels. Each inlet and outlet of microchannels was assembled with manifold parts made of Teflon, designed to sustain uniform flow distribution for each microchannel.

A schematic diagram of the experimental setup is shown in Fig. 5. It consisted of a liquid filter, liquid mass flow controller, test unit, power supply, infra-red camera, data acquisition system, and a liquid circulator included a liquid pump and liquid temperature controller unit. Deionized water was used for all the experiments and a liquid filter was placed front of the liquid circulator to prevent contaminants from flowing into the test section. The flow rate was

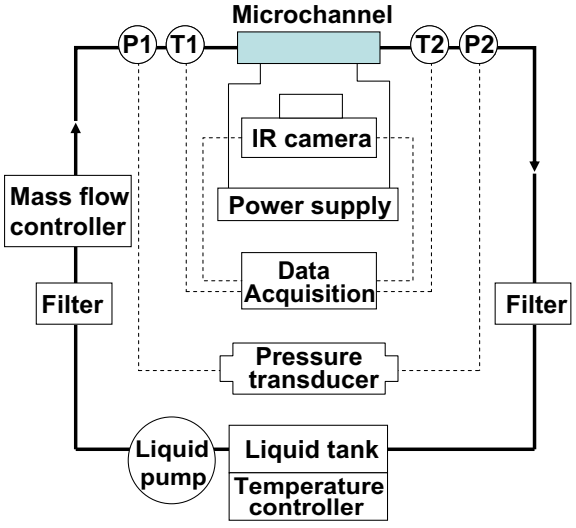

Fig. 5. Schematic diagram of test apparatus.

Table 1
Configurations of tested microchannels

(μm)	1	2	3	4	5	6	A	B	C	D
D_c	65	114	166	216	265	315	100	100	105	104
D_w	35	88	133	177	248	292	20	40	75	137
D_h	106	165	214	251	281	307	150	150	156	154
N_c	100	49	33	25	19	16	83	71	55	41
Re	69	124	194	230	230	247	77	89	113	151
	~218	~392	~519	~616	~742	~807	~241	~281	~358	~480

controlled by the liquid mass flow controller. The measurement data from pressure sensor and infra-red camera were collected by the data acquisition system.

During experimentation, each microchannel heat exchanger assembled with manifold parts was connected using inlet and outlet tubes. After setting the desired flow rate and temperature of water, electrical current was supplied to the thin film heater. When all the signals displayed on the data acquisition system reached steady-state, the experimental data were recorded. The actual supplied power was calculated from the temperature difference measured by thermocouples between inlet and outlet fluids and compared with the power from measuring the electric conditions.

An uncertainty analysis was carried out on relevant parameters using the procedure described by Holman and Gajda [21]. In this paper, the maximum values of uncertainty were dominated by the flow controller, manometer, and temperature measurement limits. The uncertainties in Reynolds number, friction factor, and Nusselt number were 2.0%, 9.2%, and 8.7%, respectively.

4. Results and discussion

4.1. Friction factor in the microchannels

The inlet and outlet manifolds are significant in measuring pressure drop and heat transfer in multiple microchannels flows [10]. Steinke and Kandlikar [5] evaluated the effect of their inlet and outlet manifolds by using loss coefficients. In this paper, we measured pressure drop more accurately by using specially designed manifolds which could induce a uniform flow distribution in the microchannels. The manifold structure shown in Fig. 6 was analyzed by using a commercially available numerical code, Fluent. From the results of numerical analysis, the optimum values of the dimensions L_c and L_b were found to be 4.5 mm and 5.5 mm, respectively. The flow rate was varied from 50 mL/min to 200 mL/min and steady-state laminar flow was assumed. Flow velocity in the microchannels ranged from 0.43 m/s to 2.6 m/s depending on the flow rate, number of channels and channel width. For 100 mL/min flow rate, the velocity distribution of inlet flow is shown in Fig. 7. The correlation coefficient of flow uniformity, obtained from statistical analysis, was 98%. The pressure drop in the manifolds as a fraction of the measured pressure drops in the microchannel ($\Delta P_{man}/\Delta P_{exp}$) was typically below 17% as shown in Fig. 8. It also shows that the fraction was less than 10% in 33 data points out of total 40 data points. In the experiments, the measured pressure data were corrected by subtracting the pressure drop of the manifolds.

The measured pressure drops with respect to Reynolds number in the microchannel are plotted in Fig. 9. Each curve was generated by varying the flow rates from 50 mL/min to 200 mL/min. It can be seen that the pressure drop is linearly proportional to the Reynolds number for a given channel width, which indicates the all the flows were laminar, without any transient effects, as predicted by classical fluid dynamic theory. The friction factors were evaluated from the experimental pressure drop data, as shown in Fig. 10. Regarding each curve, experimental data were consistent with the values predicted from the theory for fully-developed flow. Steinke and Kandlikar [5] compared previous researchers' data with their experimental results and

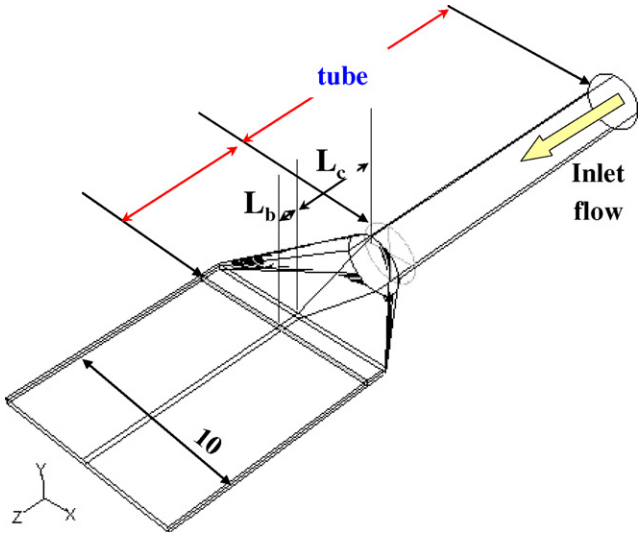

Fig. 6. Manifold structure for uniform flow distribution in the microchannel array.

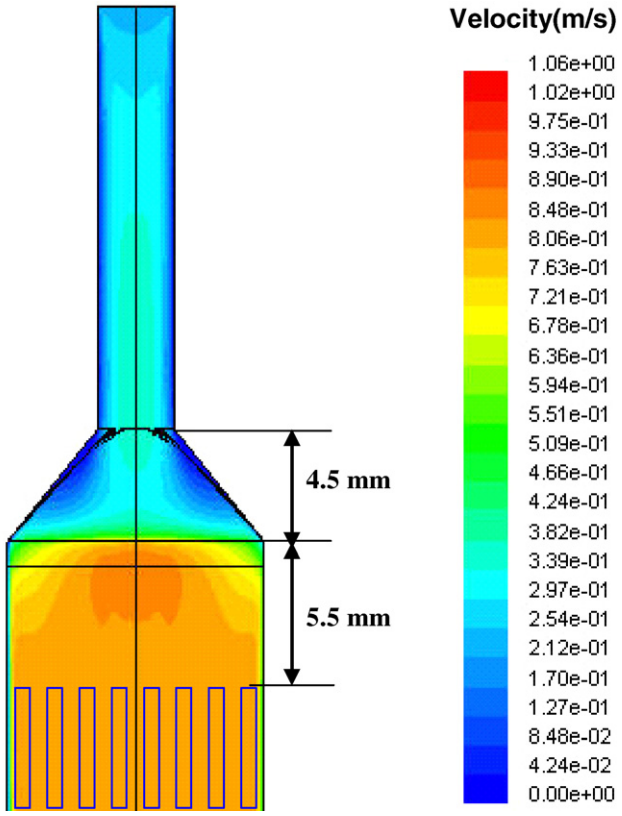

Fig. 7. Numerical calculation of flow velocity distribution in manifold.

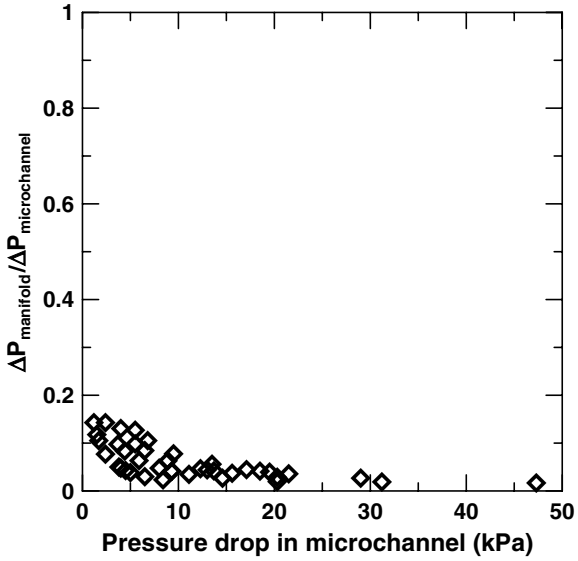

Fig. 8. Normalized pressure drops in the manifolds and the microchannels.

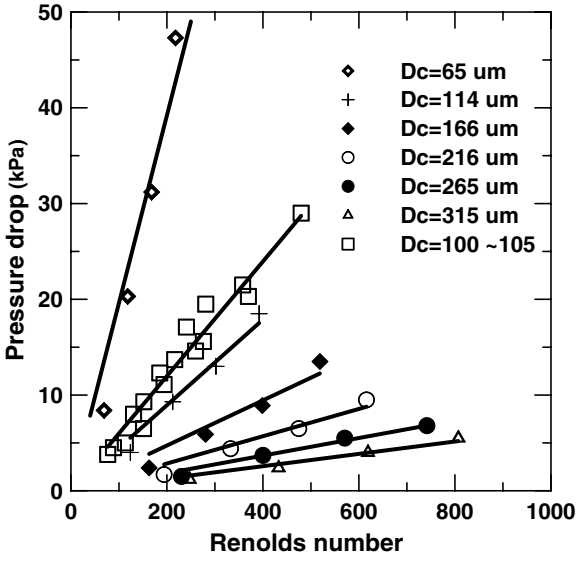

Fig. 9. Measured pressure drop as a function of Reynolds number in microchannels.

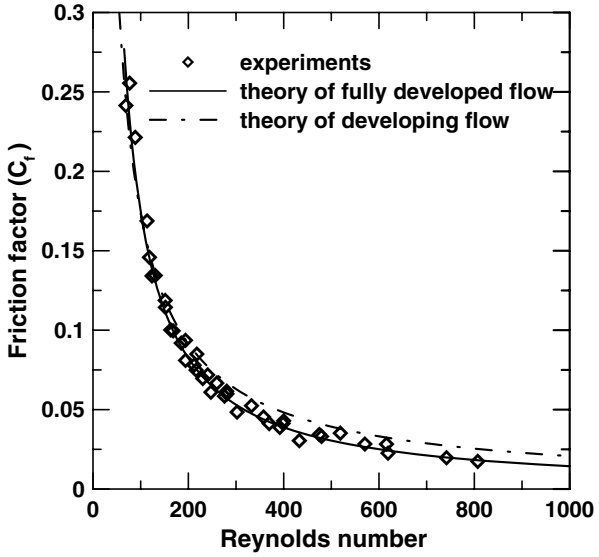

Fig. 10. A good comparison between theory and experiment.

suggested the entrance effect caused by developing flow was quite important in microchannels. However, our experimental results show the flow in the microchannels to be fully-developed. The friction factor attains 2% of its ultimate magnitude at $x^+ = 0.05$ [16]. As most of the x^+ values are bigger than 0.05 which is except for two data points (0.047 and 0.040) in our experiment, our experimental results showed good agreement with classical theory. It is thought that the friction factors in microchannel should be carefully evaluated with considering manifolds region. Fig. 11 illustrates the value of C_{f_exp}/C_{f_the} as a function of Reynolds number with comparing published data that are summarized and presented in Kohl et al. [7]. The values of C_{f_exp}/C_{f_the} obtained by assuming fully-developed flow were between 0.89 and 1.19 (average 1.03) and show that the flow in microchannels can be quite well predicted using conventional friction factor theory, and that the flow is fully-developed.

4.2. Heat transfer

The average Nusselt number was determined by using Newton's law of cooling from the measurement data

$$h = q/A(T_w - T_m) \tag{13}$$

$$A = nL(D_c + 2D_d) \tag{14}$$

A represents the fin area of cooling surface inside channels. T_w is silicon wall temperature wetted by water and this is estimated by the integrating the solution of the fin equation [10]. T_m (mean water temperature) is evaluated from averaging inlet (T_i) and outlet temperatures (T_o)

$$T_m = \frac{1}{2}(T_o - T_i) \tag{15}$$

The average Nusselt numbers derived from the experiments and theory are presented in Fig. 12. It is evident that the experimental data are scattered between the curves plotted by the theories with the assumptions of fully-developed and developed temperature profile. As the Eqs. (13)–(15) are empirical relationships obtained from macroscale flow conditions, the inconsistency is expected to be due to microscale effects.

One of the possible effects is the surface roughness which was recently studied by Croce et al. [22]. From their paper, the surface roughness was significant when the relative roughness was 2.65% to the hydraulic diameter (D_h) or Reynolds number was 1500. However, in our experiments, the surface roughness was estimated as less than 20 nm with hydraulic diameter was ranged from 106 μm to 307 μm which means that the relative roughness was from

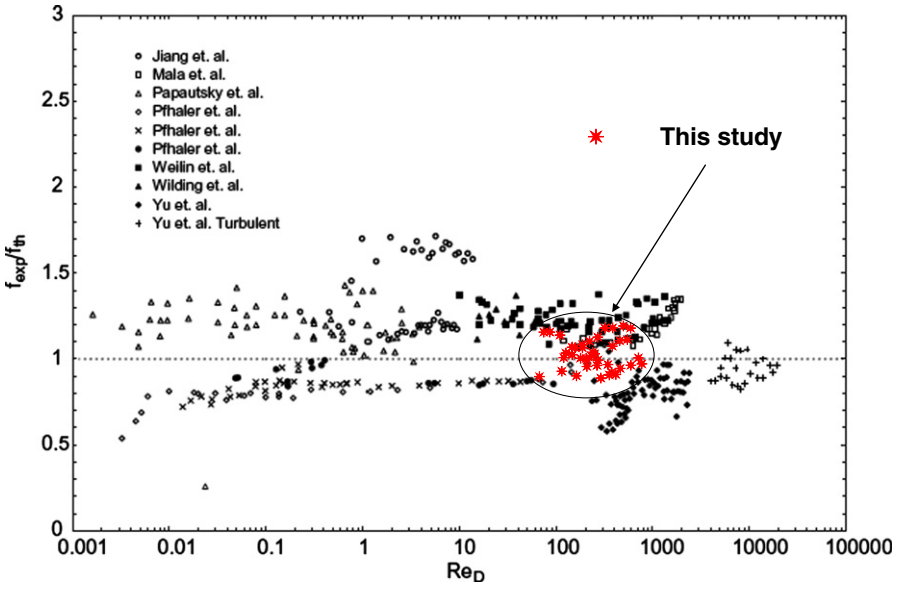

Fig. 11. The measured friction factors are compared with published data that are presented in reference paper [7].

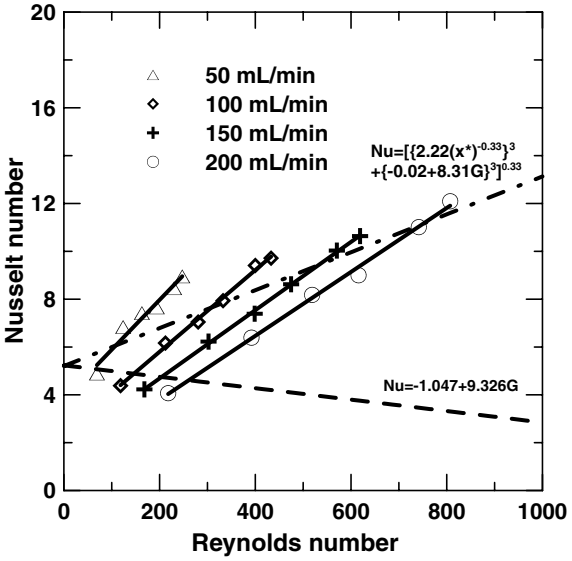

Fig. 12. Nusselt number as a function of Reynolds number.

0.007% to 0.02%. In the range, it is reasonable to neglect the surface roughness effect.

The curves plotted by Nusselt number versus Reynolds number from the experiments show different relations for each flow rate. In the heat transfer experiments, constant heat flux was applied, and the mean water temperature on the range of the flow rates varied from 28 °C to 40 °C. In this range of temperature variation, the viscosity varied 18% whereas other thermophysical properties (conductivity, heat capacity, and density) of water vary by less than 2%.

It can be deduced that flow velocity and viscosity variations cause microscale effect on the Nusselt number. In this respect, the Brinkman number is the characteristic nondimensional parameter for viscous dissipation in configurations specified in terms of heat flux [16]. In this regard, Tso and Mahulikar [13] proposed the relationship of Brinkman number with $Nu/(Re^{0.62}Pr^{0.33})$. The combined parameter of $Nu/(Re^{0.62}Pr^{0.33})$ originated from Peng et al. [14] by analyzing their experimental data and by modifying the Sieder–Tate equation [23]. They proposed a new correlation of $Nu/(Re^{0.62}Pr^{0.33})$ which features an empirical constant depending on the geometric configuration. Tso and Mahulikar [13] correlated the combined parameter with the Brinkman number in order to explain unusual behavior in the Nusselt number. Their explanations were discussed by Herwig and Hauser [24] and Hetroni et al. [12] from the physical perspective of non-realistic viscous dissipation effect in such a small Brinkman number.

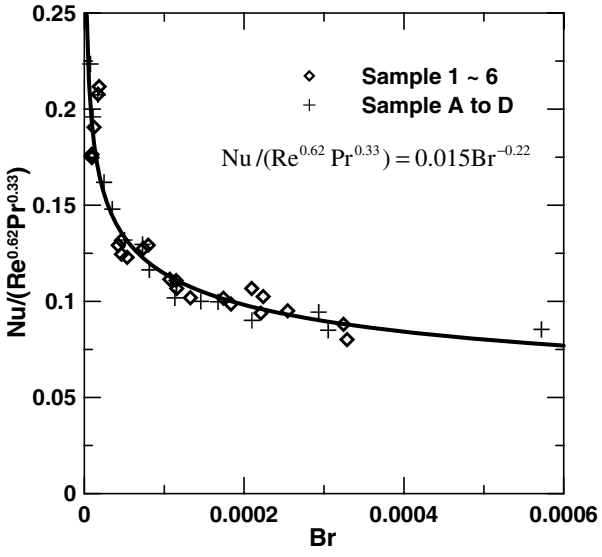

Fig. 13. $Nu/(Re^{0.62}Pr^{0.33})$ as a function of Br proposed in this paper.

However, the Brinkman number represents the relationship between viscosity and velocity in the presence of heat transfer. Our experimental data were plotted again in Fig. 13 using the new correlation and a relationship with Brinkman number was found within Prandtl number and flow velocity ranges of 4.44–5.69 and 0.34–2.61 m/s, respectively. The correlation was expressed in Eq. (16) by curve fitting from our experimental data

$$Nu/(Re^{0.62}Pr^{0.33}) = 0.015Br^{-0.22} \quad (16)$$

It showed good agreement for samples A–D those with the same hydraulic diameter of 150 μm, with different number of channels, i.e. different flow velocities in the channels. Our analysis on the experimental results for the heat transfer suggests that the Nusselt number can be predicted with accuracy using Brinkman number. Even though the correlation is related to Brinkman number, the contribution of viscous dissipation to the temperature difference between mean water and channel wall is negligible because of the low Prandtl number with low speed flow in our experiments. Hetsroni et al. [12] also concluded that the effect of viscous dissipation on heat transfer in microchannel is negligible under typical flow conditions. From the definition of Brinkman number, it implies the ratio of the momentum transfer (μV^2) to the conduction heat transfer ($k\Delta T$) across the flow. It is thought that the correlation of $Nu/(Re^{0.62}Pr^{0.33})$ and Brinkman number indicates the presence of some micro-scale effects on the heat transfer. In this regards, the slip flow effect was taken into consideration as a possible micro-scale effect. The slip flow effect contributes to decrease heat transfer rate in microchannels above the critical shear rate of 10,000 s^{-1} or 50,000 s^{-1} [25]. Fig. 14 shows the Brinkman number increases proportional to the shear rate ($6V/D_d$) which is derived by assuming parallel plates flow. As the Nusselt numbers evaluated by experiments were inversely proportional to the Brinkman number to the power of 0.22, the plotted data in Fig. 14 indicate that the heat transfer rate in the microchannels decreases with respect to the shear rate. It is inferred that the slip flow effect causes the decrease of the heat transfer rate. Further experiments are still going on in order to verify the contribution of slip flow effect on the heat transfer quantitatively.

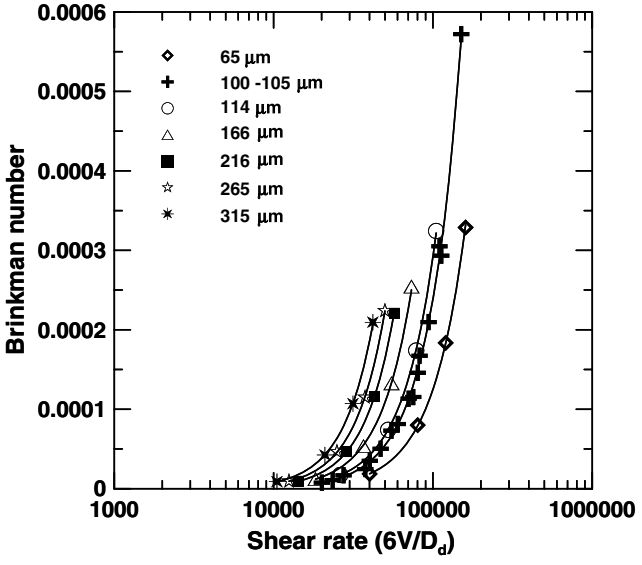

Fig. 14. Relationship of Brinkman number to the shear rate in the our experimental condition.

5. Conclusions

Friction factor and heat transfer in a range of microchannel arrays were experimentally investigated. The friction factor obtained by experiments showed excellent agreement with conventional hydraulic theory and also supported that the flow inside the microchannels was fully-developed laminar in the range of our experiments ($69 < Re < 800$ and $106\ \mu m < D_h < 307\ \mu m$). The heat transfer rates were also investigated by assuming fully-developed and developing temperature profiles. Our experimental results deviated from the Nusselt number calculated from conventional heat transfer theory. In order to predict the heat transfer rate accurately for practical applications, we proposed the correlation of $Nu/(Re^{0.62}Pr^{0.33})$ and Brinkman number which is confined to our experimental range.

References

[1] G.L. Morini, Single-phase convective heat transfer in microchannels: a review of experimental results, Int. J. Therm. Sci. 43 (2004) 631–651.
[2] N.T. Nguyen, S.T. Wereley, Artech House, Fundamentals and Applications of Microfluidics (2002), pp. 1–10.
[3] H.S. Park, J.I. Jo, J.Y. Chang, S.S. Kim, Methodology for optimization of the microchannel heat exchanger, IEEE Semiconduct. Therm. Meas., Model., Manage. Symp. (2006) 65–68.
[4] H.Y. Wu, P. Cheng, Friction factors in smooth trapezoidal silicon microchannels with different aspect ratios, Int. J. Heat Mass Transfer 46 (2003) 2519–2525.
[5] M.E. Steinke, S.G. Kandlikar, Single-phase liquid friction factors in microchannels, Int. J. Heat Mass Transfer 45 (2006) 1073–1083.
[6] J. Koo, C. Kleinstreuer, Viscous dissipation effects in microtubes and microchannels, Int. J. Heat Mass Transfer 47 (2004) 3159–3169.
[7] M.J. Kohl, S.I. Abdel-Khalik, S.M. Jeter, D.L. Sadowski, An experimental investigation of microchannel flow with internal pressure measurement, Int. J. Heat Mass Transfer 48 (2005) 1518–1533.
[8] T. Bayraktar, S.B. Pidugu, Characterization of liquid flows in microfluidic system, Int. J. Heat Mass Transfer 49 (2006) 815–824.
[9] G. Hetsroni, A. Mosyak, Z. Segal, G. Ziskind, A uniform temperature heat sink for cooling of electronic devices, Int. J. Heat Mass Transfer 45 (2002) 3275–3286.
[10] T.M. Harms, M.J. Kazmierczak, F.M. Gerner, Developing convective heat transfer in deep rectangular microchannels, Int. J. Heat Mass Transfer 20 (1999) 149–167.
[11] P.S. Lee, S.V. Garimella, D. Liu, Investigation of heat transfer in rectangular microchannels, Int. J. Heat Mass Transfer 48 (2005) 1688–1704.
[12] G. Hetsroni, A. Mosyak, E. Pogrebnyak, L.P. Yarin, Heat transfer in micro-channels: comparison of experiments with theory and numerical results, Int. J. Heat Mass Transfer 48 (2005) 5580–5601.
[13] C.P. Tso, S.P. Mahulikar, Experimental verification of the role of Brinkman number in microchannels using local parameters, Int. J. Heat Mass Transfer 43 (2000) 1837–1849.

[14] X.F. Peng, G.P. Peterson, B.X. Wang, Heat transfer characteristics of water flowing through microchannels, Exp. Heat Transfer 7 (1994) 265–283.
[15] F.M. White, Fluid Mechanics, third ed., McGraw-Hill, 1994.
[16] W.M. Kays, M.E. Crawford, Convective Heat and Mass Transfer, third ed., McGraw-Hill, 1993.
[17] A. Bejan, Convection Heat Transfer, Wiley, 1990.
[18] R.W. Knight, D.J. Hall, J.S. Goodling, R.C. Jaeger, Heat sink optimization with application to microchannels, IEEE Trans. Compon., Hybr., Manufact. Technol. 15 (1992) 832–842.
[19] D. Copeland, Optimization of parallel plate heatsinks for forced convection, in: 16th IEEE SEMI-THERM Symposium, 2000, pp. 266–272.
[20] R.K. Shah, A.L. London, Laminar flow forced convection in ducts, Adv. Heat Transfer (Suppl. 1) (1978).
[21] J.P. Holman, W.J. Gajda, Experimental Methods for Engineers, fifth ed., Mcgraw-Hill, 1989.
[22] G. Croce, P. D'agaro, C. Nonino, Three-dimensional roughness effect on microchannel heat transfer and pressure drop, Int. J. Heat Mass Transfer 50 (2007) 5249–5259.
[23] E.N. Sieder, G.E. Tate, Heat transfer and pressure drop of liquids in tubes, Ind. Eng. Chem. 28 (1936) 1435–1492.
[24] H. Herwig, O. Hausner, Critical view on new results in micro-fluid mechanics: an example, Int. J. Heat Mass Transfer 46 (2003) 935–937.
[25] G. Rosengarten, J. Cooper-White, G. Metcalfe, Experimental and analytical study of the effect of contact angle on liquid convective heat transfer in microchannels, Int. J. Heat Mass Transfer 49 (2006) 4161–4170.